

# KU ScholarWorks

## Search for CP violation in D(0) decay

Item Type	Article
Authors	Baringer, Philip S.
Citation	J. Bartelt et al. [1995]. "Search for CP violation in D(0) decay." Physical Review D, 52(9):4860. <a href="http://dx.doi.org/10.1103/PhysRevD.52.4860">http://dx.doi.org/10.1103/PhysRevD.52.4860</a>
DOI	<a href="http://dx.doi.org/10.1103/PhysRevD.52.4860">10.1103/PhysRevD.52.4860</a>
Publisher	American Physical Society
Download date	2024-07-30 10:54:44
Link to Item	<a href="http://hdl.handle.net/1808/15310">http://hdl.handle.net/1808/15310</a>

**Search for  $CP$  violation in  $D^0$  decay**

J. Bartelt, S.E. Csorna, Z. Egyed, and V. Jain  
*Vanderbilt University, Nashville, Tennessee 37235*

D. Gibaut, K. Kinoshita, and P. Pomianowski  
*Virginia Polytechnic Institute and State University, Blacksburg, Virginia 24061*

B. Barish, M. Chadha, S. Chan, D.F. Cowen, G. Eigen, J.S. Miller, C. O'Grady, J. Urheim, A.J. Weinstein,  
and F. Würthwein  
*California Institute of Technology, Pasadena, California 91125*

D.M. Asner, M. Athanas, D.W. Bliss, W.S. Brower, G. Masek, and H.P. Paar  
*University of California, San Diego, La Jolla, California 92093*

J. Gronberg, C.M. Korte, R. Kutschke, S. Menary, R.J. Morrison, S. Nakanishi, H.N. Nelson, T.K. Nelson, C. Qiao,  
J.D. Richman, D. Roberts, A. Ryd, H. Tajima, and M.S. Witherell  
*University of California, Santa Barbara, California 93106*

R. Balest, K. Cho, W.T. Ford, M. Lohner, H. Park, P. Rankin, and J.G. Smith  
*University of Colorado, Boulder, Colorado 80309-0390*

J.P. Alexander, C. Bebek, B.E. Berger, K. Berkelman, K. Bloom, T.E. Browder,\* D.G. Cassel, H.A. Cho,  
D.M. Coffman, D.S. Crowcroft, M. Dickson, P.S. Drell, D.J. Dumas, R. Ehrlich, R. Elia, P. Gaidarev,  
M. Garcia-Sciveres, B. Gittelman, S.W. Gray, D.L. Hartill, B.K. Heltsley, S. Henderson, C.D. Jones, S.L. Jones,  
J. Kandaswamy, N. Katayama, P.C. Kim, D.L. Kreinick, T. Lee, Y. Liu, G.S. Ludwig, J. Masui, J. Mevissen,  
N.B. Mistry, C.R. Ng, E. Nordberg, J.R. Patterson, D. Peterson, D. Riley, and A. Soffer  
*Cornell University, Ithaca, New York 14853*

P. Avery, A. Freyberger, K. Lingel, J. Rodriguez, S. Yang, and J. Yelton  
*University of Florida, Gainesville, Florida 32611*

G. Brandenburg, D. Cinabro, T. Liu, M. Saulnier, R. Wilson, and H. Yamamoto  
*Harvard University, Cambridge, Massachusetts 02138*

T. Bergfeld, B.I. Eisenstein, J. Ernst, G.E. Gladding, G.D. Gollin, M. Palmer, M. Selen, and J.J. Thaler  
*University of Illinois, Champaign-Urbana, Illinois 61801*

K.W. Edwards, K.W. McLean, and M. Ogg  
*Carleton University, Ottawa, Ontario, Canada K1S 5B6*  
*and the Institute of Particle Physics, Canada*

A. Bellerive, D.I. Britton, E.R.F. Hyatt, R. Janicek, D.B. MacFarlane, P.M. Patel, and B. Spaan  
*McGill University and the Institute of Particle Physics, Montréal, Québec, Canada H3A 2T8*

A.J. Sadoff  
*Ithaca College, Ithaca, New York 14850*

R. Ammar, P. Baringer, A. Bean, D. Besson, D. Coppage, N. Coptly, R. Davis, N. Hancock, M. Kelly, S. Kotov,  
I. Kravchenko, N. Kwak, and H. Lam  
*University of Kansas, Lawrence, Kansas 66045*

Y. Kubota, M. Lattery, M. Momayezi, J.K. Nelson, S. Patton, R. Poling, V. Savinov, S. Schrenk, and R. Wang  
*University of Minnesota, Minneapolis, Minnesota 55455*

---

\*Permanent address: University of Hawaii at Manoa.

M.S. Alam, I.J. Kim, Z. Ling, A.H. Mahmood, J.J. O'Neill, H. Severini, C.R. Sun, and F. Wappler  
*State University of New York at Albany, Albany, New York 12222*

G. Crawford, R. Fulton, D. Fujino, K.K. Gan, K. Honscheid, H. Kagan, R. Kass, J. Lee, M. Sung, C. White,  
 A. Wolf, and M.M. Zoeller  
*Ohio State University, Columbus, Ohio 43210*

X. Fu, B. Nemati, W.R. Ross, P. Skubic, and M. Wood  
*University of Oklahoma, Norman, Oklahoma 73019*

M. Bishai, J. Fast, E. Gerndt, J.W. Hinson, R.L. McIlwain, T. Miao, D.H. Miller, M. Modesitt, D. Payne,  
 E.I. Shibata, I.P.J. Shipsey, and P.N. Wang  
*Purdue University, West Lafayette, Indiana 47907*

L. Gibbons, Y. Kwon, S. Roberts, and E.H. Thorndike  
*University of Rochester, Rochester, New York 14627*

T. Coan, J. Dominick, V. Fadeyev, I. Korolkov, M. Lambrecht, S. Sanghera, V. Shelkov, T. Skwarnicki,  
 R. Stroynowski, I. Volobouev, and G. Wei  
*Southern Methodist University, Dallas, Texas 75275*

M. Artuso, M. Gao, M. Goldberg, D. He, N. Horwitz, G.C. Moneti, R. Mountain, F. Muheim, Y. Mukhin,  
 S. Playfer, Y. Rozen, S. Stone, X. Xing, and G. Zhu  
*Syracuse University, Syracuse, New York 13244*

(CLEO Collaboration)  
 (Received 22 May 1995)

Using  $2.7 \text{ fb}^{-1}$  of data taken with the CLEO II detector, we have searched for  $CP$  violation in the charm system. We looked for asymmetries in the number of decays of  $D^0$ 's and  $\bar{D}^0$ 's to the  $CP$  eigenstates  $K^+K^-$ ,  $K_S^0\phi$ , and  $K_S^0\pi^0$ . Confidence intervals (90%) on these asymmetries were found to be  $-0.020 < A_{KK} < 0.180$ ,  $-0.182 < A_{K_S^0\phi} < 0.126$ , and  $-0.067 < A_{K_S^0\pi^0} < 0.031$ , respectively.

PACS number(s): 13.25.Ft, 11.30.Er

## I. INTRODUCTION

To date, the only experimental evidence for  $CP$  violation is found in the kaon system. Here we report on a search for  $CP$  violation in the charm system. We look for an asymmetry in the decay rates of  $D^0$  and  $\bar{D}^0$  mesons to  $CP$  eigenstates. This asymmetry is defined as

$$A = \frac{\Gamma(D^0) - \Gamma(\bar{D}^0)}{\Gamma(D^0) + \Gamma(\bar{D}^0)},$$

where  $\Gamma(D^0)$  and  $\Gamma(\bar{D}^0)$  are the partial decay widths of the  $D^0$  and  $\bar{D}^0$  into the same  $CP$  eigenstate.

In this paper, we study decays to the following  $CP$  eigenstates:  $K^+K^-$ ,  $K_S^0\phi$ , and  $K_S^0\pi^0$ . We use the fact that for the decay modes

$$D^{*+} \rightarrow D^0 + \pi^+$$

and

$$D^{*-} \rightarrow \bar{D}^0 + \pi^-$$

the charge of the pion tags the flavor of the  $D^0(\bar{D}^0)$ , and assume equal production of  $D^{*+}$  and  $D^{*-}$ . The  $D$

decay widths are proportional to the yields up to a very small correction for an asymmetry in detection efficiency described later.

Within the standard model, the asymmetry for the  $D^0 \rightarrow K^+K^-$  mode is at most a few  $10^{-3}$  [1].  $CP$  asymmetries at the percent level are quite conceivable for the  $D^0 \rightarrow K_S^0\pi^0$  and  $D^0 \rightarrow K_S^0\phi$  modes if there are contributions from new physics such as nonminimal supersymmetry [1,2]. Recent publications from the E691 Collaboration [3] and the E687 Collaboration [4] report upper limits on the  $CP$  asymmetry for the  $K^+K^-$  mode of  $A_{KK} < 0.45$  and  $-0.11 < A_{KK} < 0.16$ , respectively, at the 90% confidence level. We know of no published experimental upper limits for the  $D^0 \rightarrow K_S^0\phi$  and  $D^0 \rightarrow K_S^0\pi^0$  modes.

## II. THE ANALYSIS

### A. Data sample

We use  $2.7 \text{ fb}^{-1}$  of data taken with the CLEO II detector [5] at the Cornell Electron Storage Ring (CESR). These data were taken at center-of-mass energies of 10.58

and 10.52 GeV on and just below the  $\Upsilon(4S)$  resonance. The detector components important for this analysis are a tracking system consisting of a six-layer straw tube chamber, a ten-layer vertex drift chamber, and a 51-layer main drift chamber, and an electromagnetic calorimeter consisting of 7800 CsI crystals, all operating inside a 1.5-T solenoidal magnet. The typical impact parameter resolution in the tracking detector is between 0.1 and 0.2 mm in  $r\phi$ . The measured momentum resolution of the tracking system is given by  $\sigma_p^2/p^2 = (0.0050)^2 + (0.0015)^2 p^2$ , where  $p$  is in GeV/c. The track reconstruction efficiency at low momentum rises with momentum above the tracking threshold of 65 MeV/c and passes through 50% at a momentum of 100 MeV/c. We identify particles based upon specific ionization ( $dE/dx$ ) information from the main drift chamber [5].

## B. Measurements

### 1. $D^0(\bar{D}^0) \rightarrow K^+K^-$

The first decay mode we have studied is  $D^0(\bar{D}^0) \rightarrow K^+K^-$ . We form  $D^0$ 's by combining tracks whose specific ionization is consistent with the kaon hypothesis. We then pair this  $D^0$  candidate with a pion to form a  $D^*$ , whose charge tags the flavor of the  $D$ . We refer to this pion as the ‘‘soft pion.’’

This mode has background from  $D^0(\bar{D}^0) \rightarrow K^\mp\pi^\pm$  decays. Though the reconstructed masses of these events lie above the signal region, they can make background subtraction more difficult. In order to select the  $K^+K^-$  decay mode and reduce the  $K\pi$  background, we require that the normalized difference between the expected and measured  $dE/dx$  for the kaon hypothesis be within  $3\sigma$  for both kaon tracks. Since we know whether we have a  $D^0$  or  $\bar{D}^0$  decay we can identify the charge of the track most likely to be a pion if we were misreconstructing this decay. We therefore require that  $dE/dx$  of this candidate kaon be more than  $1.5\sigma$  away from the mean for a pion. To further reduce the background, we require that the absolute value of the cosine of the angle between the  $K^\pm$  momentum in the  $D^0$  rest frame and the  $D^0$  laboratory momentum ( $|\cos\theta_{K^\pm}|$ ) be less than 0.8. Since the  $D^0$  is spinless it decays isotropically, whereas the background peaks at  $|\cos\theta_{K^\pm}| \approx 1.0$ . We also require that the momentum of each kaon be greater than 0.3 GeV/c. Finally, we impose a  $D^0$  momentum cut of  $P_{D^0} > 1.7$  GeV/c in order to reduce the background from random track combinations which accidentally give the correct mass.

We select  $D^*$ 's by requiring that the reconstructed mass difference,  $\Delta M (\equiv M_{D^{*+}} - M_{D^0})$  lies within 1.4 MeV/c<sup>2</sup> ( $\sim 2\sigma$ ) of the nominal mass difference of 145.4 MeV/c<sup>2</sup> (Figs. 1 and 2). In addition to the fact that the soft pion tags the flavor of the  $D^0$  or  $\bar{D}^0$  meson, this cut strongly suppresses the background coming from random combinations of tracks which accidentally give the expected masses. We define the signal region to be within  $3\sigma$  of the fitted mass, determined using a Gaussian fit to the combined  $K^+K^-$  mass distribution shown in Fig. 3. For this channel the signal region is between 1.84 and

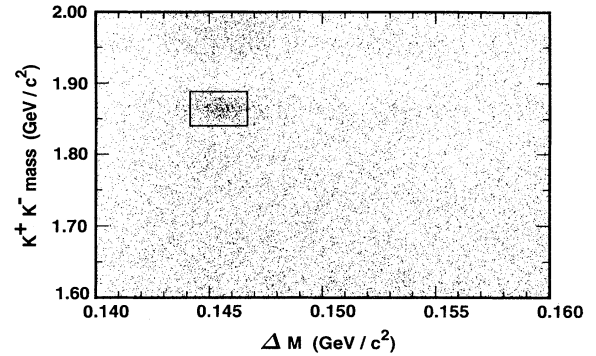


FIG. 1. The reconstructed  $K^+K^-$  invariance mass vs the  $D^{*+} - D^0$  mass difference distribution after all of cuts for  $K^+K^-$  for  $D^0$  and  $\bar{D}^0$  combined. The box shows the signal region for both  $D^0(\bar{D}^0)$  mass and mass difference distribution.

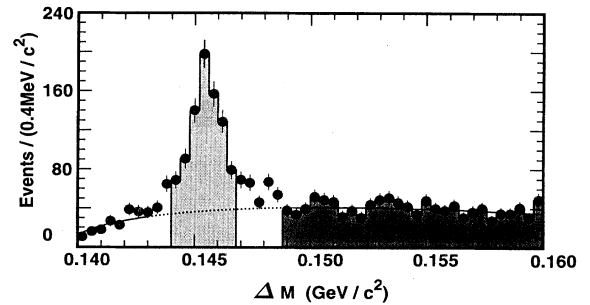


FIG. 2. The mass difference distribution after all of cuts for  $K^+K^-$  for  $D^0$  and  $\bar{D}^0$  combined. The lighter shaded area represents the signal region and the darker shaded area represents the sideband region. The solid curve is a phase space background function described in the text which is fit in the regions  $0.1400 \leq \Delta M \leq 0.1430$  GeV/c<sup>2</sup> and  $0.1488 \leq \Delta M \leq 0.1600$  GeV/c<sup>2</sup>.

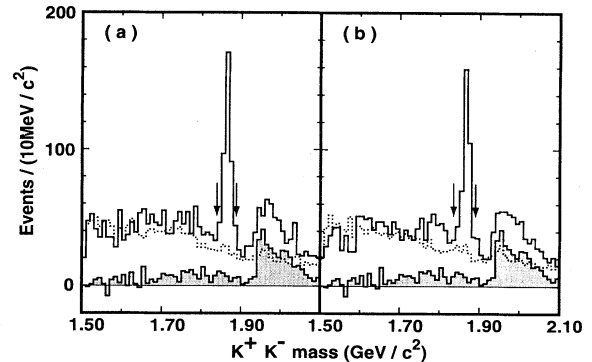


FIG. 3. (a) The reconstructed  $D^0$  mass spectrum for  $D^0 \rightarrow K^+K^-$ . (b) The reconstructed  $\bar{D}^0$  mass spectrum for  $\bar{D}^0 \rightarrow K^+K^-$ . The solid line is the  $D^0(\bar{D}^0)$  mass signal in the mass difference signal region. The dotted line is background from the mass difference sideband region. The shaded area represents the background from the other charm decay modes, which is calculated by Monte Carlo events after doing the  $\Delta M$  sideband subtraction. We see the peak around 1.98 GeV/c<sup>2</sup> due to the misidentified  $D^0(\bar{D}^0) \rightarrow K^\mp\pi^\pm$  events. The arrows show the signal region.

1.89  $\text{GeV}/c^2$ . The number of events lying in the  $\Delta M$  signal region and within the  $D^0(\bar{D}^0)$  signal region is 449 (414).

In most of the background events, a wrong soft pion was used to form the  $D^*$ . We determine the number of these events by fitting the  $\Delta M$  background distribution and integrating under the curve in the signal region as shown in Fig. 2. The functional form used is

$$a(\Delta M - m_{\pi^+})^{0.5} + b(\Delta M - m_{\pi^+})^{1.5} + c(\Delta M - m_{\pi^+})^{2.5},$$

where the first term is from a nonrelativistic model of phase space, and the second and third terms are the first and second order relativistic corrections to the nonrelativistic model, respectively. The asymmetry is insensitive to the details of the background fitting method. We make a simultaneous fit to the  $D^0$  and  $\bar{D}^0$  data to determine the shape of the background function but allow separate normalizations. The normalization factor comes from the ratio between integrating under the curve in the signal region and in the sideband region in the  $\Delta M$  plot. The number of background events in the  $D^0$  signal region is  $129 \pm 6 \pm 6$  and the number in the  $\bar{D}^0$  signal region is  $135 \pm 6 \pm 7$  where the first error comes from the statistics in the sideband regions, which determine the background normalization, and the second error comes from the statistical uncertainty in the background shape. Since we determine these numbers by scaling the  $\Delta M$  sideband contributions, the statistical errors are smaller than the square root of the number of events. We have checked that the ratio of events in the signal to sideband regions is the same for the  $D^0$  and  $\bar{D}^0$  samples using the high statistics  $D^0 \rightarrow K^\mp \pi^\pm$  mode. While the absolute background levels differ slightly, this ratio is the same within errors.

At this stage, there is the possibility that backgrounds from other charm decay modes such as  $K^\mp \pi^\pm \pi^0$  are also present in the  $D$  signal region even if most of these events lie outside the  $D$  signal region. To determine this background, we use a Monte Carlo simulation of continuum hadron production and decay followed by a full simulation of the signals the particles produced in the detector. The  $K^+K^-$  invariant mass distribution of these events excluding true  $D^0(\bar{D}^0) \rightarrow K^+K^-$  decays is shown superimposed on the data in Fig. 3, where the background from the  $\Delta M$  sideband was subtracted for Monte Carlo events. The normalization of the simulated events is absolutely determined from the luminosity. As shown in Fig. 4, the backgrounds are well understood. We find  $31 \pm 8$  background events from this source, which we assume to be the same for the  $D^0$  and  $\bar{D}^0$  samples. After subtracting all the backgrounds, we find  $N_{K^+K^-} = 289 \pm 23 \pm 6$  for  $D^0 \rightarrow K^+K^-$  and  $N_{K^+K^-} = 248 \pm 23 \pm 7$  for  $\bar{D}^0 \rightarrow K^+K^-$ , where the first error is statistical and the second error is the correlated error due to the statistical uncertainties in the background shapes.

## 2. $D^0(\bar{D}^0) \rightarrow K_S^0 \phi$

To reconstruct the  $D^0(\bar{D}^0) \rightarrow K_S^0 \phi$  decay mode, we first reconstruct  $K_S^0$  mesons from  $\pi^+\pi^-$  pairs with an

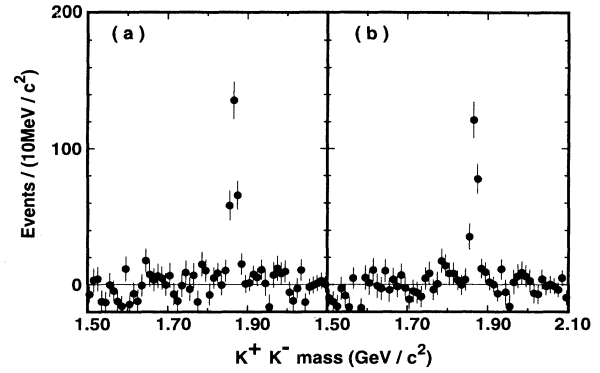


FIG. 4. (a) The reconstructed  $D^0$  mass spectrum for  $D^0 \rightarrow K^+K^-$  after subtracting all the backgrounds. (b) The reconstructed  $\bar{D}^0$  mass spectrum for  $\bar{D}^0 \rightarrow K^+K^-$  after subtracting all the backgrounds.

invariant mass within  $0.012 \text{ GeV}/c^2$  ( $\sim 3\sigma$ ) of the nominal  $K_S^0$  mass and a vertex displaced at least 1 mm from the beam position. We reconstruct the  $\phi$  via its  $K^+K^-$  decay mode. The  $K^+$  and  $K^-$  tracks must have specific ionization in the drift chamber within  $2\sigma$  of that expected for kaons. The  $K^+K^-$  mass spectrum is shown in Fig. 5. Candidate  $\phi$  decays lie in the mass range  $1.012 < M_{K^+K^-} < 1.028 \text{ GeV}/c^2$ .

To subtract the background to the  $\phi$ , we extrapolate under the  $\phi$  peak, assuming that the background level varies linearly with  $M_{K^+K^-}$ . We find 36 (37) background events in the  $D^0(\bar{D}^0)$  sample, where the  $D^0$  and  $\bar{D}^0$  samples have been separated using the charge of the pion from the  $D^*$  decay. We have checked that other

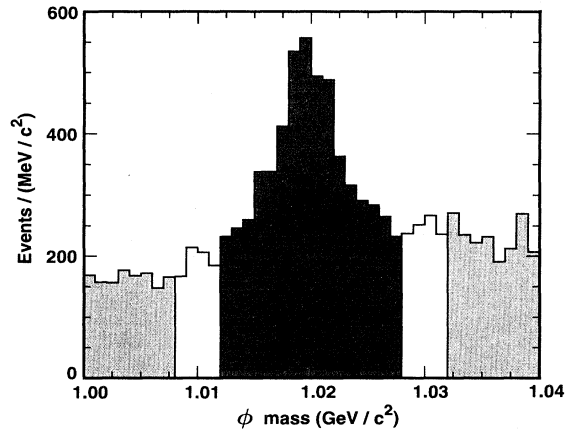


FIG. 5.  $\phi$  mass spectrum for  $\phi \rightarrow K^+K^-$  after passing particle ID cuts. The darker shaded area represents the signal region and the lighter shaded areas represent the sideband regions. We will use these sideband regions to remove nonresonant  $M_{K_S^0 K^+K^-}$  background in  $M_{K_S^0 \phi}$  plots.

<sup>1</sup>Note this non- $\phi$  background includes nonresonant  $K_S^0 K^+K^-$  production, which is not a definite  $CP$  eigenstate.

functional forms for the background give results consistent with this.

The  $K_S^0\phi$  invariant mass spectra are shown in Fig. 6. In these plots, the non- $\phi$  background distribution has been taken from the  $M_{K^+K^-}$  sidebands and subtracted. We then proceed as in the previous decay mode. For this channel the signal region is between 1.85 and 1.89  $\text{GeV}/c^2$ . The number of events in the  $D^0$  signal region is  $143\pm 15$  and the number in the  $\bar{D}^0$  signal region is  $146\pm 15$ . The number of  $D^0$  background events from the mass difference sideband region is  $26\pm 4\pm 7$  and the number of  $\bar{D}^0$  background events is  $21\pm 4\pm 6$ , where the first error comes from the statistics in the sideband regions, which determine the background normalization, and the second error comes from the statistical uncertainty in the background shape. No Monte Carlo simulated events from other charm decay modes appear in the  $D^0(\bar{D}^0)$  mass signal region.

Finally, the background subtracted  $K_S^0\phi$  invariant mass distributions are shown in Fig. 7. We obtain  $N_{K_S^0\phi} = 117\pm 16\pm 7$  for  $D^0 \rightarrow K_S^0\phi$  and  $\bar{N}_{K_S^0\phi} = 125\pm 16\pm 6$  for  $\bar{D}^0 \rightarrow K_S^0\phi$ , where the first error is statistical and the second error is the correlated error due to the statistical uncertainties in the background shapes.

### 3. $D^0(\bar{D}^0) \rightarrow K_S^0\pi^0$

We next consider the mode  $D^0(\bar{D}^0) \rightarrow K_S^0\pi^0$ . We detect  $\pi^0$ 's by their decays to  $\gamma\gamma$ . Candidate  $\pi^0$ 's are formed by taking two-photon combinations. The energy of each photon cluster candidate in the CsI calorimeter has to be at least 30 MeV and the diphoton combination must have at least one photon in the higher resolution portion of the calorimeter ( $|\cos(\theta)| < 0.71$ , where  $\theta$  is the angle with respect to the beam axis). We reject all clusters matched to charged tracks in the central detector.

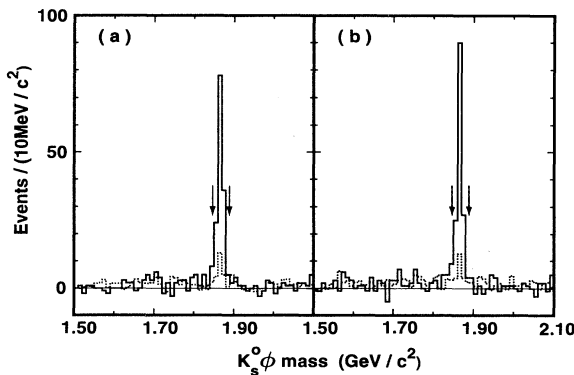


FIG. 6. (a) The reconstructed  $D^0$  mass spectrum for  $D^0 \rightarrow K_S^0\phi$ . (b) The reconstructed  $\bar{D}^0$  mass spectrum for  $\bar{D}^0 \rightarrow K_S^0\phi$ . In this  $D^0(\bar{D}^0)$  mass signal, we use  $\phi$  sideband subtraction in order to remove nonresonant  $K_S^0 K^+ K^-$  background. The solid line is the  $D^0(\bar{D}^0)$  mass signal in the mass difference signal region. The dotted line is background from the mass difference sideband region. The arrows show the signal region.

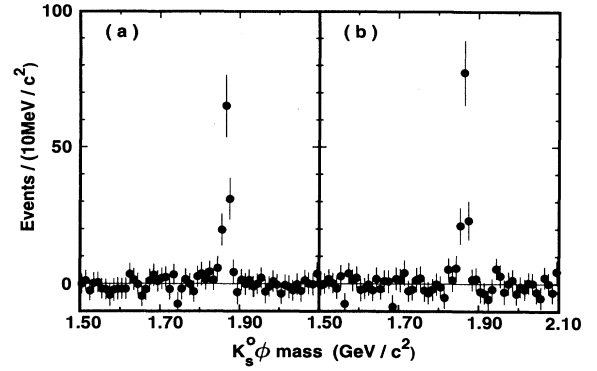


FIG. 7. (a) The reconstructed  $D^0$  mass spectrum for  $D^0 \rightarrow K_S^0\phi$  after subtracting the background. (b) The reconstructed  $\bar{D}^0$  mass spectrum for  $\bar{D}^0 \rightarrow K_S^0\phi$  after subtracting the background.

We require that the momentum of the diphoton combination be greater than 0.2  $\text{GeV}/c$  and that the mass of this combination be within  $2\sigma$  ( $\sim 10 \text{ MeV}/c^2$ ) of the pion mass.

In addition to the  $K_S^0$  cuts used in the  $K_S^0\phi$  analysis, we require  $|\cos\theta_{K_S^0}| < 0.8$  where  $\theta_{K_S^0}$  is the angle between the  $K_S^0$  momentum in the  $D^0$  rest frame and the  $D^0$  laboratory momentum. We also impose a  $D^0$  momentum cut of  $P_{D^0} > 1.7 \text{ GeV}/c$ .

Using these cuts we obtain the  $K_S^0\pi^0$  mass spectra shown in Fig. 8. For this channel the signal region is between 1.80 and 1.92  $\text{GeV}/c^2$ . The number of events in the  $D^0$  signal region is 773 and the number in the  $\bar{D}^0$  signal region is 796. The number of background events after  $\Delta M$  sideband scaling in the  $D^0$  signal region is  $97\pm 4\pm 6$  and the number in the  $\bar{D}^0$  signal region is  $90\pm 4\pm 5$ , where the first error comes from the statistics in the sideband

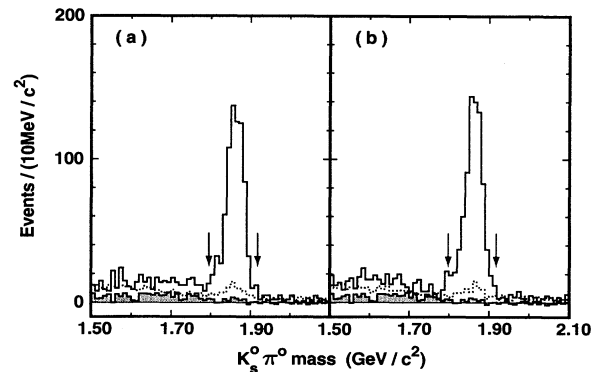


FIG. 8. (a) The reconstructed  $D^0$  mass spectrum for  $D^0 \rightarrow K_S^0\pi^0$ . (b) The reconstructed  $\bar{D}^0$  mass spectrum for  $\bar{D}^0 \rightarrow K_S^0\pi^0$ . The solid line is the  $D^0(\bar{D}^0)$  mass signal in the mass difference signal region. The dotted line is background from the mass difference sideband region. The arrows show the signal region. The shaded area represents the background from other charm decay modes, which is calculated by Monte Carlo events after doing the  $\Delta M$  sideband subtraction.

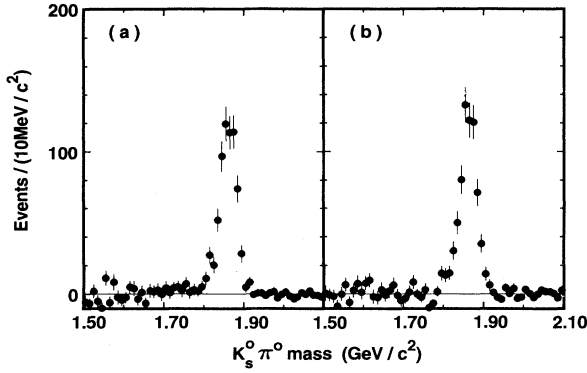


FIG. 9. (a) The reconstructed  $D^0$  mass spectrum for  $D^0 \rightarrow K_S^0 \pi^0$  after subtracting all the backgrounds. (b) The reconstructed  $\bar{D}^0$  mass spectrum for  $\bar{D}^0 \rightarrow K_S^0 \pi^0$  after subtracting all the backgrounds.

regions, which determine the background normalization, and the second error comes from the statistical uncertainty in the background shape. No Monte Carlo simulated events from other charm decay modes appear in the  $D^0(\bar{D}^0)$  mass signal region. After subtracting the backgrounds as shown in Fig. 9, we find  $N_{K_S^0 \pi^0} = 676 \pm 28 \pm 6$  for  $D^0 \rightarrow K_S^0 \pi^0$  and  $\bar{N}_{K_S^0 \pi^0} = 706 \pm 28 \pm 5$  for  $\bar{D}^0 \rightarrow K_S^0 \pi^0$ , where the first error is statistical and the second error is the correlated error due to the statistical uncertainties in the background shapes.

$$4. \quad \overset{(-)}{D^0} \rightarrow K^\mp \pi^\pm$$

Finally we search for an asymmetry in the  $\overset{(-)}{D^0} \rightarrow K^\mp \pi^\pm$  mode. This study checks the analysis, particularly the

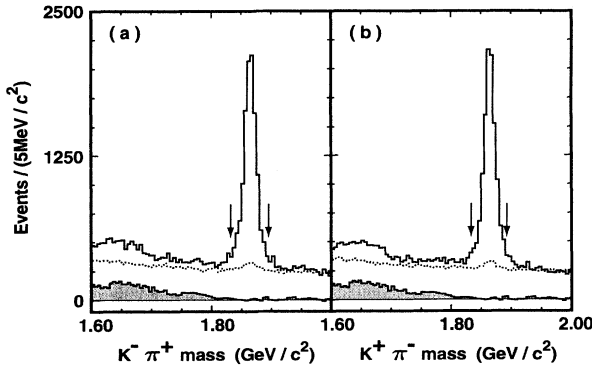


FIG. 10. (a) The reconstructed  $D^0$  mass spectrum for  $D^0 \rightarrow K^- \pi^+$ . (b) The reconstructed  $\bar{D}^0$  mass spectrum for  $\bar{D}^0 \rightarrow K^+ \pi^-$ . The solid line is the  $D^0(\bar{D}^0)$  mass signal in the mass difference signal region. The dotted line is background from the mass difference sideband region. The shaded area represents the background from the other charm decay modes, which is calculated by Monte Carlo events after doing the  $\Delta M$  sideband subtraction.

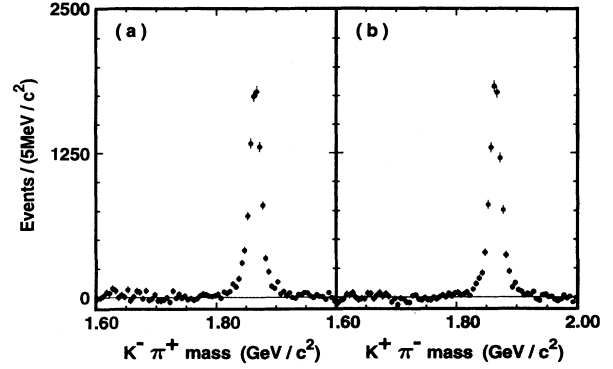


FIG. 11. (a) The reconstructed  $D^0$  mass spectrum for  $D^0 \rightarrow K^- \pi^+$  after subtracting all the backgrounds. (b) The reconstructed  $\bar{D}^0$  mass spectrum for  $\bar{D}^0 \rightarrow K^+ \pi^-$  after subtracting all the backgrounds.

equivalence of our finding efficiency for soft  $\pi^+$  and  $\pi^-$  tracks. However, the interpretation of the results from this check depends on the assumption that  $CP$  violation is negligible for this mode, as predicted in the standard model. If nonstandard model effects contribute, then the rates for each decay may not be the same. This asymmetry measurement can therefore be interpreted either as a systematic check or as a limit on  $CP$  violation.

Given the charge of the soft pion, we consider same-sign charged tracks as pions and opposite-sign charged tracks as kaons, when finding  $D^0(\bar{D}^0)$  candidates. Then, we select events by requiring the  $D^0$  momentum be greater than 1.7 GeV/c and the momenta of the kaon and pion which reconstruct the  $D^0(\bar{D}^0)$  be greater than 0.3 GeV/c.

Using these cuts we obtain the  $K^\mp \pi^\pm$  mass spectra shown in Fig. 10. For this channel the signal re-

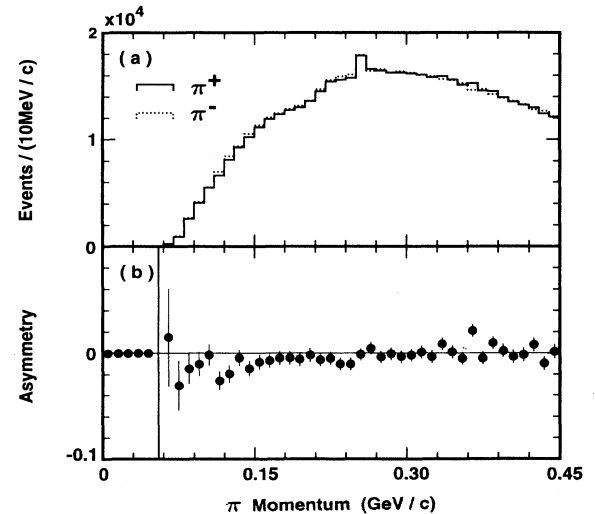


FIG. 12. (a) The soft  $\pi$  momentum distributions in  $K_S^0 \rightarrow \pi^+ \pi^-$ . We see an excess of events at 0.25 GeV/c (approximately half of  $K_S^0$  mass) due to very low momentum of  $K_S^0$ . (b) The asymmetry vs  $\pi$  momentum in  $K_S^0 \rightarrow \pi^+ \pi^-$ .

TABLE I. The systematic error on the asymmetry due to differences in soft pion detection efficiency.

Channel	Shift in asymmetry $A \pm dA$
$\bar{D}^0 \rightarrow K^+ K^-$	$-0.004 \pm 0.006$
$D^0 \rightarrow K_S^0 \phi$	$-0.005 \pm 0.007$
$D^0 \rightarrow K_S^0 \pi^0$	$-0.004 \pm 0.006$

gion lies between 1.835 and 1.895 GeV/ $c^2$ . The number of events in the  $D^0$  signal region is 12 734 and the number in the  $\bar{D}^0$  signal region is 12 644. The number of  $D^0$  background events from the scaled mass difference sideband region is  $3542 \pm 26 \pm 32$  and the number of  $\bar{D}^0$  background events is  $3394 \pm 25 \pm 31$ , where the first error comes from the statistics in the sideband regions, which determine the background normalization, and the second error comes from the statistical uncertainty in the background shape. Other charm decay modes such as  $K^\mp \pi^\pm \pi^0$  contribute  $85 \pm 28$  events. After subtracting all the backgrounds as shown in Fig. 11, we obtain  $N_{K^-\pi^+} = 9107 \pm 119 \pm 32$  for  $D^0 \rightarrow K^-\pi^+$  and  $\bar{N}_{K^+\pi^-} = 9165 \pm 119 \pm 31$  for  $\bar{D}^0 \rightarrow K^+\pi^-$ , where the first error is statistical and the second error is the correlated error due to the statistical uncertainties in the background shapes.

From these numbers we obtain the measured asymmetry  $A = -0.003 \pm 0.009$ . Finally, after compensating for the systematic bias between the  $\pi^+$  and  $\pi^-$  detection efficiencies described in the next section, we obtain  $A_{K\pi} = 0.001 \pm 0.011$  or  $-0.017 < A_{K\pi} < 0.019$  at the 90% confidence level [6].

### C. Systematic studies

Since the assumption that there are equal numbers of  $D^{*\pm}$ 's produced and detected is crucial to this analysis, we have searched for systematic biases which would give an asymmetry in the number of  $D^{*+}$  and  $D^{*-}$  reconstructed. The most probable source of a bias is a difference in the efficiencies for detecting positive and negative soft pions. We have checked for this effect in several ways.

#### 1. Beam pipe interaction

Since the soft pions we detect have traveled through a beryllium beam pipe [5], a difference in the hadronic interactions for negative and positive pions would cause an asymmetry. Isospin arguments show that any such difference would come from a difference in the number of protons and neutrons in the beam pipe. We have calculated the interaction probabilities in all of the materials between the interaction point and the drift chamber and find that the fractional difference in rates is less than 0.0004. This is negligible given the size of our statistical error.

TABLE II. The results.

Channel	$CP$ asymmetry	90% confidence range [6]
$\bar{D}^0 \rightarrow K^+ K^-$	$0.080 \pm 0.061$	$-0.020 < A_{KK} < 0.180$
$D^0 \rightarrow K_S^0 \phi$	$-0.028 \pm 0.094$	$-0.182 < A_{K_S^0 \phi} < 0.126$
$D^0 \rightarrow K_S^0 \pi^0$	$-0.018 \pm 0.030$	$-0.067 < A_{K_S^0 \pi^0} < 0.031$

### 2. Soft $\pi$ detection efficiency

To look directly for differences in the reconstruction efficiencies of soft pions we use pions from  $K_S^0$  decays. The procedure is to determine the number of  $\pi^+$  and  $\pi^-$  bin by bin in pion momentum and calculate the asymmetry  $A(p)$  in each bin of pion momentum defined as

$$A(p) = \frac{N_{\pi^+} - N_{\pi^-}}{N_{\pi^+} + N_{\pi^-}},$$

where  $N_{\pi^+}(N_{\pi^-})$  is the number of soft  $\pi^+(\pi^-)$ . Note that while this study is insensitive to a momentum-independent asymmetry in the detection efficiencies, studies have shown that it is a good measure of asymmetries that affect only low momentum tracks.

After selecting a clean sample of  $K_S^0$ 's decaying within the beam pipe, we obtain the soft  $\pi$  momentum distributions shown in Fig. 12(a). These soft  $\pi$  momentum distributions yield the bin-by-bin asymmetry shown in Fig. 12(b). There is evidence for a small bias in the momentum region of interest between 0.10 and 0.25 GeV/ $c$ . To obtain an appropriate correction for each mode, we fold this asymmetry into the momentum spectrum of the soft pions from  $D^*$  decay. Table I shows these corrections.

## III. RESULTS

The final results are shown in Table II. We see no evidence for  $CP$  violation in any of these channels. The results shown here for the  $D^0 \rightarrow K_S^0 \phi$  and  $D^0 \rightarrow K_S^0 \pi^0$  modes represent the first limits on  $CP$  violation in these channels. The  $D^0 \rightarrow K^+ K^-$  result is comparable to that from other experiments [4].

## ACKNOWLEDGMENTS

We gratefully acknowledge the effort of the CESR staff in providing us with excellent luminosity and running conditions. This work was supported by the National Science Foundation, the U.S. Department of Energy, the Heisenberg Foundation, the Alexander von Humboldt Stiftung, the Natural Sciences and Engineering Research Council of Canada, and the A.P. Sloan Foundation.



- [1] I. I. Bigi, in *Proceedings of the Tau-Charm Factory Workshop*, Stanford, California, 1989, edited by Lydia V. Beers (SLAC Report No. 343, Stanford, 1989), p. 169; Report No. UND-HEP-94-BIG11, 1994 (unpublished).
- [2] I. I. Bigi, F. Gabbiani, and A. Masiero, *Z. Phys. C* **48**, 633 (1990).
- [3] J. C. Anjos *et al.*, *Phys. Rev. D* **44**, R3371 (1991).
- [4] P. L. Frabetti *et al.*, *Phys. Rev. D* **50**, R2953 (1994).
- [5] Y. Kubota *et al.*, *Nucl. Instrum. Methods Phys. Res. Sect. A* **320**, 66 (1992).
- [6] We center this interval on our measured value.

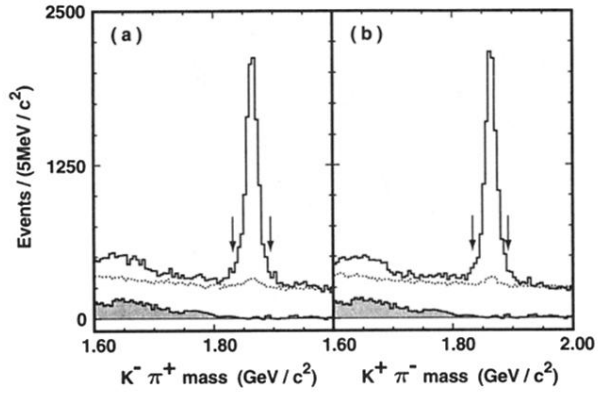


FIG. 10. (a) The reconstructed  $D^0$  mass spectrum for  $D^0 \rightarrow K^- \pi^+$ . (b) The reconstructed  $\bar{D}^0$  mass spectrum for  $\bar{D}^0 \rightarrow K^+ \pi^-$ . The solid line is the  $D^0$  ( $\bar{D}^0$ ) mass signal in the mass difference signal region. The dotted line is background from the mass difference sideband region. The shaded area represents the background from the other charm decay modes, which is calculated by Monte Carlo events after doing the  $\Delta M$  sideband subtraction.

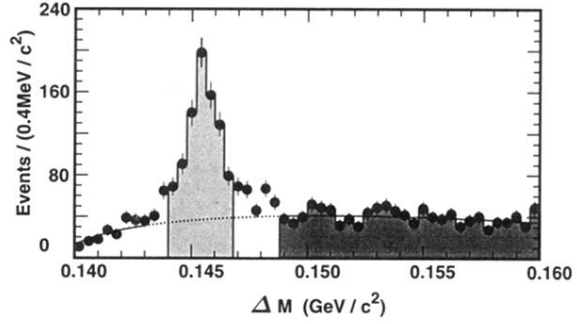


FIG. 2. The mass difference distribution after all of cuts for  $K^+K^-$  for  $D^0$  and  $\bar{D}^0$  combined. The lighter shaded area represents the signal region and the darker shaded area represents the sideband region. The solid curve is a phase space background function described in the text which is fit in the regions  $0.1400 \leq \Delta M \leq 0.1430 \text{ GeV}/c^2$  and  $0.1488 \leq \Delta M \leq 0.1600 \text{ GeV}/c^2$ .

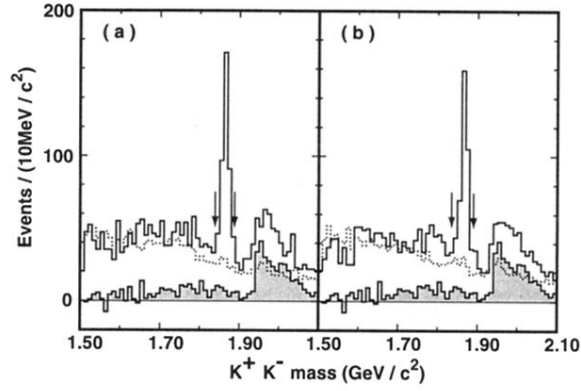


FIG. 3. (a) The reconstructed  $D^0$  mass spectrum for  $D^0 \rightarrow K^+K^-$ . (b) The reconstructed  $\bar{D}^0$  mass spectrum for  $\bar{D}^0 \rightarrow K^+K^-$ . The solid line is the  $D^0(\bar{D}^0)$  mass signal in the mass difference signal region. The dotted line is background from the mass difference sideband region. The shaded area represents the background from the other charm decay modes, which is calculated by Monte Carlo events after doing the  $\Delta M$  sideband subtraction. We see the peak around 1.98  $\text{GeV}/c^2$  due to the misidentified  $D^0(\bar{D}^0) \rightarrow K^\mp\pi^\pm$  events. The arrows show the signal region.

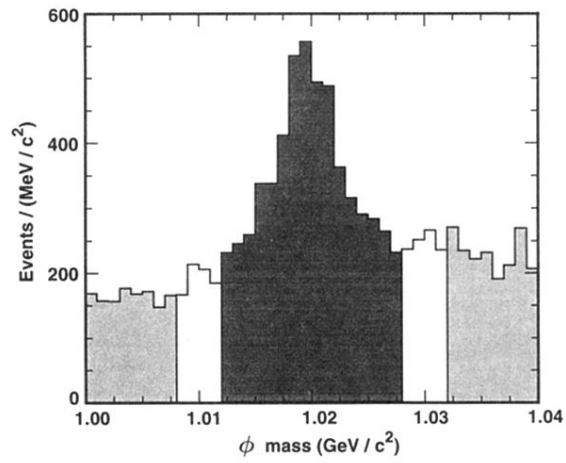


FIG. 5.  $\phi$  mass spectrum for  $\phi \rightarrow K^+K^-$  after passing particle ID cuts. The darker shaded area represents the signal region and the lighter shaded areas represent the sideband regions. We will use these sideband regions to remove non-resonant  $M_{K_S^0 K^+ K^-}$  background in  $M_{K_S^0 \phi}$  plots.

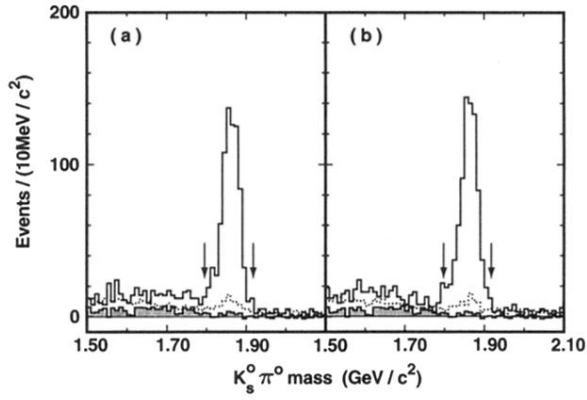


FIG. 8. (a) The reconstructed  $D^0$  mass spectrum for  $D^0 \rightarrow K_S^0 \pi^0$ . (b) The reconstructed  $\bar{D}^0$  mass spectrum for  $\bar{D}^0 \rightarrow K_S^0 \pi^0$ . The solid line is the  $D^0$  ( $\bar{D}^0$ ) mass signal in the mass difference signal region. The dotted line is background from the mass difference sideband region. The arrows show the signal region. The shaded area represents the background from the other charm decay modes, which is calculated by Monte Carlo events after doing the  $\Delta M$  sideband subtraction.